www.czasopisma.pan.pl PAN POLSKA AKADEMIA NAUK www.journals.pan.pl

Arch. Min. Sci. **64** (2019), 2, 447-461

Electronic version (in color) of this paper is available: http://mining.archives.pl

DOI 10.24425/ams.2019.128694

ANDRZEJ TRUTY*#, ZENON PILECKI**, KRZYSZTOF STYPUŁA*,
RAFAŁ WIŚNIOWSKI***, KRZYSZTOF KOZIOŁ*, STANISŁAW STRYCZEK***

ASSESSMENT OF GROUND VIBRATIONS INDUCED BY GAS AND OIL WELL DRILLING USING NUMERICAL SIMULATIONS

OCENA DRGAŃ GRUNTU WYWOŁANYCH WIERCENIEM OTWORÓW POSZUKIWAWCZYCH GAZU/ROPY NAFTOWEJ Z WYKORZYSTANIEM SYMULACJI NUMERYCZNEJ

This work presents the methodology for analyzing the impact of ground vibrations induced during the drilling of gas/oil exploration wells on the surrounding constructions, as well as on humans and the natural environment. In the primary stage, this methodology is based on measurements of ground vibrations induced by a specific type of drilling system in the so-called reference site. In the next stage, ground vibrations are estimated in similar conditions to another design site, these conditions are assumed for a given drilling system, treated as a vibration source. In both sites, special seismic and geotechnical data are collected to construct numerical models for dynamic analyses. Finally, if it is required, a protection system is proposed with respect to the drilling technology and local conditions. The methodology presented has been tested on the terrain of an active natural gas mine used as the design site, and located in the southeastern part of Poland. The reference site was placed in the terrain of a working drilling system in similar conditions in the central part of Poland. Based on the results of numerical simulations, one may verify the different locations of the drilling rig in the design site with respect to the existing industrial structure. Due to the hazard from destructive ground vibrations, a certain vibroisolation system was proposed at the design site. Based on the results of numerical simulations one could rearrange the components of the drilling system in order to provide maximum security for the surrounding structures.

Keywords: ground vibrations, gas/oil drilling rigs, FEM simulations, vibroisolations

W pracy przedstawiono, składającą się z kilku etapów, metodykę oceny wpływu drgań podłoża indukowanych w trakcie wiercenia otworów poszukiwawczych gazu/ropy na znajdujące się w pobliżu obiekty budowlane i infrastrukturę, ludzi a także środowisko naturalne. W pierwszym etapie wykonywane są pomiary drgań podłoża generowane przez system wiercący danego typu w tzw. miejscu referencyjnym. Jest to na ogół miejsce, w którym dany system wiercący jest aktualnie używany. Następnie szacowane

* CRACOW UNIVERSITY OF TECHNOLOGY, WARSZAWSKA 24, 31-155 KRAKÓW, POLAND
** MINERAL AND ENERGY ECONOMY RESEARCH INSTITUTE POLISH ACADEMY OF SCIENCES, WYBICKIEGO 7A, 31-261 KRAKÓW, POLAND
*** AGH UNIVERSITY OF SCIENCE AND TECHNOLOGY, MICKIEWICZA 30, 30-059 KRAKÓW, POLAND
\# Corresponding author: andrzej.truty@gmail.com

są drgania wywołane przez dany system wiercący w miejscu nowo projektowanego otworu poszukiwawczego. W obydwu miejscach wykonywane są specjalistyczne badania sejsmiczne i geotechniczne w celu opracowania oraz wykalibrowania modeli numerycznych dla opisu propagacji drgań wywołanych pracą systemu wiercącego. W przypadku, gdy jest to niezbędne, dla nowego otworu poszukiwawczego, projektowany jest system wibroizolacyjny, którego celem jest istotna redukcja amplitud drgań w podłożu. Przedstawiona w pracy metodyka została przetestowana na terenie czynnej kopalni gazu ziemnego zlokalizowanej w południowo-wschodniej części Polski, na terenie której planowany był nowy otwór. Miejsce referencyjne zostało wybrane w centralnej części Polski gdzie odbywały się prace wiertnicze w podobnych warunkach geologiczno-inżynierskich do tych odpowiadających lokalizacji nowo projektowanego otworu. Na podstawie wyników symulacji numerycznych MES zweryfikowano położenie platformy wiertniczej w miejscu nowo projektowanego otworu względem istniejącej infrastruktury przemysłowej. Ze względu na zagrożenie destrukcyjnym wpływem drgań zaprojektowano i zweryfikowano specjalny system wibroizolacji. Opracowana metodyka umożliwia ocenę wpływu drgań podłoża przez systemy wiercące oraz optymalizację ich położenia tak aby zapewnić maksymalne bezpieczeństwo otaczającym konstrukcjom.

Słowa kluczowe: drgania gruntu, wiertnie gazu/ropy naftowej, symulacje MES, wibroizolacje

1. Introduction

The drilling of gas/oil wells in the neighborhood of existing industrial or building structures is a challenging task in engineering practice. Working drilling systems may generate ground vibrations which have a dynamic impact, not only on the surrounding structures, but also on humans and the natural environment.

The basic source of vibrations in conventional oil/gas well drilling is rotary motion of the drilling rig component, conveyed to the drill-string and drill-bit (Jardine et al., 1994).

A typical drilling rig performs three major functions (Spanos et al., 2003): it accommodates the vertical motion of the drill-string, rotates the drilling assembly, and circulates the drilling fluid. The necessary equipment for these operations includes the derrick and the hoisting system, the rotary table and the kelly, and the mud pumps, respectively. The dynamic behavior of the drilling system depends on many components, including the drilling rig rotated parts (surface rotation), drill string bouncing and rotating and bottom hole assemblies (BHA) vibrations (Saldivar et al., 2014; Saldivar Marquez et al., 2015).

As reported by Spanos et al. (2003) different kinds of drilling vibration measurements may be traced to the early 1960s (Finnie & Bailey, 1960; Bailey & Finnie, 1960; Angona, 1965; Cunningham, 1968; Miller & Rollins, 1968). These measurements were generally based on vibration minimization for a given set of operating parameters, or the optimal operating parameters were predicted for a given BHA configuration (Bailey et al., 2008). Since then, both measurement techniques and equipment have improved, but the dynamic impact on the environment is only reported very rarely. Nicholls (2009) presented the results of vibration monitoring during different drilling activities at a number of sites. The data set were typically gathered at distances of between 5 m and 50 m from the drilling rig. It was noticeable for some activities that, at a distance of 50 m, the vibration was deemed negligible. The results confirm that the chiseling associated with cable percussion drilling gives rise to the highest level of vibration. In conditions of weathered Sherwood sandstone strata, vibration levels with a peak particle velocity (PPV) associated with chiseling of 2.5 10^{-3} m/sec occur in close proximity (10 m) to the drilling rig (Fig. 1). The presented data points signify the possibility of a significant drop in vibration intensity occurring at or about 15 m from the drilling rig. In Fig. 1, the exponential regression was calculated for measurement points placed a minimum of 15 m from the borehole.

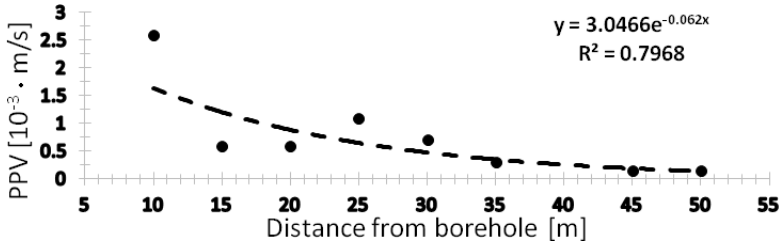

Fig. 1. Vibration associated with chiseling on Sherwood Sandstone bedrock (after Nicholls, 2009)

Measurements of ground vibrations at a distance of at least 20 meters from the working drilling rig could assess their impact on the environment. By doing this one could check the parameter changes of the ground vibrations in a far field from the drilled well, where the influence of different interfering factors is limited. Such information would be also sufficient to optimize the location of the drilling rig from the structures and if necessary, to design a protection system (Stypuła, 1981). However, certain technological, as well as economic aspects determine that such an "ex post" formulated approach cannot usually be used in all conditions. When the drilling process is running, it is very difficult to design and construct an efficient protection system at that stage. Before drilling starts, one should be equipped with sufficiently comprehensive knowledge concerning the expected dynamic impact on the surrounding structures, and also on humans and the natural environment.

This work presents the methodology of the estimation of ground vibrations impact induced by the drilling rig on surrounding structures as illustrated by the example of its application on the terrain of an active natural gas mine (named ZL), used as a design site, and located in southeastern part of Poland. In this area, the need to perform a drilling well caused certain technological limitations related to the dynamic impact on neighboring mine industrial installations. Another research terrain (named BEL) was considered as a reference site in comparison with the working drilling system, the same one to be used at the design site, placed in the central part of Poland. For an assessment of the influence of ground vibrations, Finite Element Method (FEM) simulations were carried out on the basis of data provided by seismic measurements, and also based on available geotechnical data describing the structure and dynamic properties of the subsurface geological medium at both, reference and design sites.

2. Methodology

The general methodology consists of two major investigation stages (IS) and three stages of analysis (AS). In the first IS stage, at both sites, the reference and design one, special seismic investigations are conducted to the obtain dynamic parameters of the near surface medium and its lithology. These investigations include performing refraction seismic measurements to determine the structure and dynamic properties of the near surface medium along the profile of further ground acceleration measurements, but also gathering available archival geotechnical information concerning the structure and dynamic properties of the geological medium. In the second IS stage, ground vibrations induced by a given type of drilling system, in the reference site, are measured. These measurements include the maximal amplitudes of the vertical and ra-

dial components of acceleration at a given distance from the working drilling system. Based on these measurements the attenuation coefficient and also the frequency range of the signal, with dominant frequencies, are estimated.

On the basis of the collected data, numerical simulations are then carried out in three main AS stages. In the stage AS-I – scale factor s is numerically back-analyzed in order to calibrate the signal induced by working drilling rig at the reference site. This scale factor s is applied to the inertia forces resulting from the mass of the rig and vertical acceleration time history $a_z(t)$ measured at a point located on the drilling rig. All dynamic back-analyses are carried out in time domain using simplified axisymmetric FEM models, described in a detailed manner in chapters 3.2 and 3.3. To minimize the computation error and maintain control of the damping in the numerical model, the Hilber – Hughes –Taylor (HHT) integration scheme (Hilber et al., 1977) is used. In the stage AS-II the calibrated signal is transferred to the conditions of the design site to generate free field motion. If it is deemed necessary a certain set of vibroisolation systems is considered at this stage and new free field motion fields are computed. In stage AS-III – the dynamic impact of ground vibrations induced by the drilling rig on neighboring structures is analyzed, at the design site, using the Domain Reduction Method (DRM) (Bielak et al. 2003, Youshimura et al. 2003), implemented in the ZSoil code (Truty & Zimmermann, 2013). In the context of the DRM method and the analyzed problem of the influence of ground vibrations on the structure, a simplified axisymmetric FEM analysis of the free field motion (induced by the drilling rig), is carried out first. In the second step, a reduced 3D model of a structure and a relatively small adjacent part of the subsoil is analyzed using previously computed free field motion (Fig. 2). The spatial domain in the reduced 3D model is divided into three zones i.e. the interior domain which includes the structure and part of the adjacent subsoil (it may be nonlinear in general), boundary zone (single layer of elastic elements) and the exterior domain (also single layer of elastic elements) in which decomposition of the total motion into the free field and the residual one is used (see Appendix 1 for more details).

In order to study the effect of the distance between the drilling rig and a given structure it is enough to geometrically shift all nodes of the reduced 3D model mesh in the radial direction.

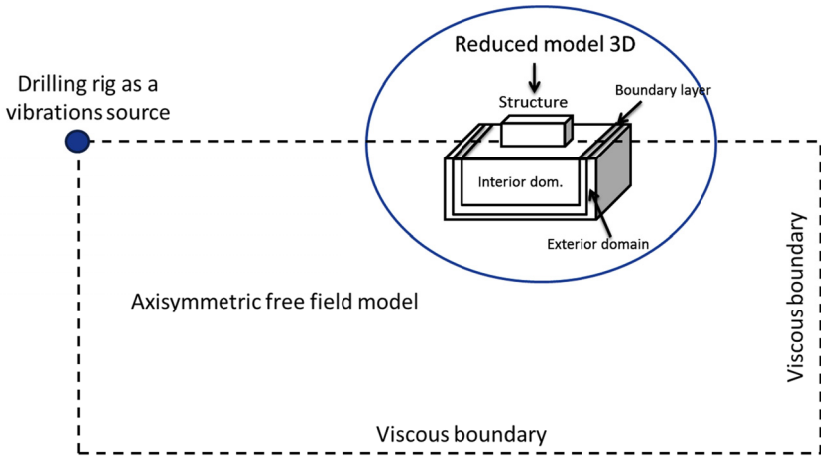

Fig. 2. General scheme of the Domain Reduction Method

The main role of the boundary layer is to transfer the signal from the free field to the interior zone. As is shown in Appendix 1 the only nonzero terms in the right hand side vector (eq. A 1.7) of the discrete FE system, appear at the nodes of elements in the boundary layer.

Based on these simulations one may verify the different locations of the working drilling rig in the design site with respect to the neighboring structures. The minimal distance of the drilling rig from the structure is one of the major design parameters. If the minimal distance is too large, simulations are repeated with the use of the vibroisolation system. It is possible to analyse the possible location of components of the drilling rig to provide maximal safety for the surrounding structures. In this way one can optimize the drilling process against the unfavorable impact of ground vibrations not only on the surrounding structures, but also on humans and the environment.

3. Modelling of the vibrations influence on surrounding structures

3.1. General information

The use of the Skytop TR-800 type of drilling rig with a mass of about 28 000 kg was designed on the terrain of the natural gas ZL mine. Ground vibrations generated by the same type of working drilling rig were measured from the reference site (BEL) in similar geological conditions, in loose quaternary sediments. Furthermore, in both sites, seismic refraction measurements were conducted to estimate the dynamic properties and near surface structure of the geological medium. Some available archival information about the structure and properties of the geological medium were also collected.

In order to quantitatively assess the influence of designed ground vibrations on the existing industrial installation of the natural gas ZL mine (Fig. 3) a simplified 3D dynamic FEM analysis along with the methodology presented in section 2 was carried out. It is assumed that the drilling rig is located at a distance of 28 m from a selected installation segment. Numerical simulations were performed with use of ZSoil PC.2013 and DIANA software.

Fig. 3. The analyzed segment of the mine installation (ZL)

3.2. Modelling of ground vibrations generated by the drilling rig in the BEL reference site

The reference site, near the surface medium consists of: sand of about 0-14 m, clay of about 15-20 m, and deeper sand. The results of seismic refraction measurements indicated a horizontal and undisturbed course of seismic borders (Report, 2012). Around the drilling rig in a radius of about 12 m, reinforced concrete plates 30 cm thick were installed. The values of the acceleration components registered in the source amounted to 1.15 m/s^2 for the V (vertical) component, 0.97 m/s^2 for the T (transverse) component, and 1.36 m/s^2 for the R (radial) component, but in the far field, from 20 m from the borehole they did not exceed 0.18 m/s^2 (Fig. 4). The calculated attenuation coefficient value for the far field was 0.015 for vertical acceleration and 0.013 for radial acceleration.

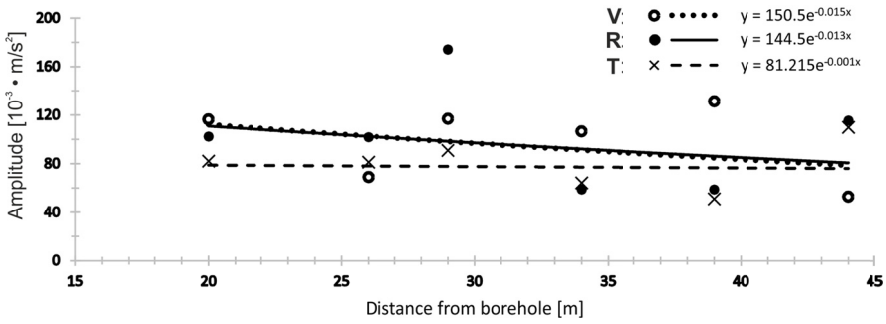

Fig. 4. Acceleration amplitude components vs. distance from the working Skytop TR-800 type of drilling rig in the reference site (V – vertical, R – radial, T – transversal)

The geometry of the FEM model consisted of the first two layers (the deeper layer of sand did not influence the results) and reinforced concrete plates placed on top of them (Fig. 5). The calculation mesh of quadrilateral elements of size h = 0.4 m was established. The bottom frame of the model was not fixed, only viscous dashpots were added there. The Dynamic Young modulus E and Poisson ratio ν of these layers were estimated based on the results of seismic refraction measurements. The Rayleigh damping coefficients α_o and β_o were obtained as a result of numerical simulations. The calculation time step was equal to Δt = 0.0009765 s. The Hilber-Hughes-Taylor (HHT) scheme was used to integrate equations of motion in the time domain. The measured and calculated dynamic parameters of the layers and concrete plates in the reference site are presented in Table 1.

TABLE 1

Parameters of geological layers and concrete plate in the reference site (BEL)

No. of layer	Type of material	E [MPa]	v [-]	γ [kN/m^3]	α_o [1/s]	β_o [s]
1	Sand	744	0.454	19	0.241	$6.12 \cdot 10^{-5}$
2	Clay	1338	0.440	20	0.241	$6.12 \cdot 10^{-5}$
3	Concrete plate	30000	0.2	25	0.241	$6.12 \cdot 10^{-5}$

The drilling rig was represented by two lumped masses m_i = 1 400 kg, and the sum of them is equal to the total mass 28 000 kg. Nodal forces $F_i(t)$, concentrated at two nodal points (Fig. 5) were applied:

$$F_i(t) = s\, m_i\, a_z(t) \tag{1}$$

where:

s — scale factor,
m_i — lumped mass,
$a_z(t)$ — vertical acceleration.

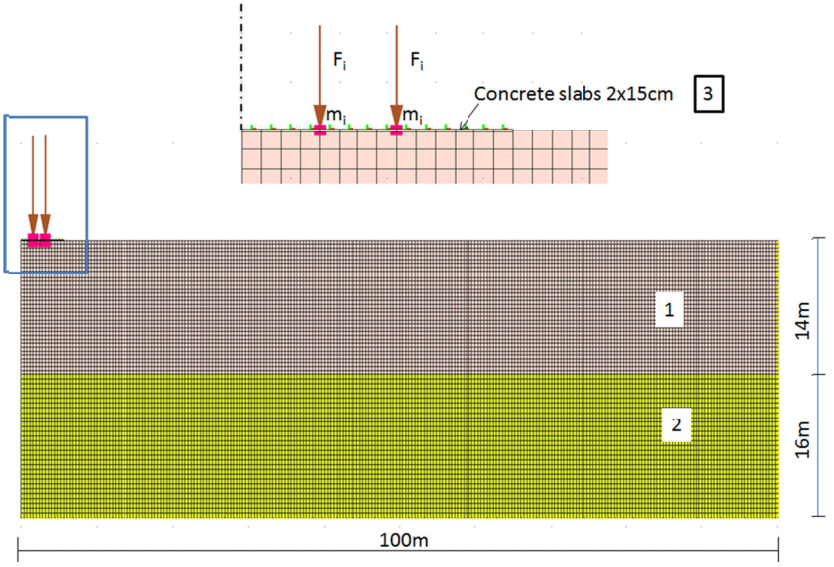

Fig. 5. Geometry of the axisymmetric model with applied forces for the reference site (BEL)

The $a_z(t)$ was measured at the point of the vibration source on the drilling rig in the reference site. The applied signal $a_z(t)$, before simulation, was low pass filtered with a 120 Hz cut-off frequency (Fig. 6a, 6b). Higher frequency content does not have a harmful influence on the mine installation, but it may introduce numerical errors. The scale factor s was estimated to equalize measured and computed radial acceleration amplitudes at distances larger than 20 m from the source.

It is well known, that the Rayleigh model yields frequency dependent values of the attenuation coefficient ξ. Therefore, a Fourier analysis of the dominant frequencies of recorded signals indicated that the band 30-100 Hz was the most interesting one. Hence, Rayleigh parameters (α_o, β_o) were estimated assuming a constant value of attenuation coefficient $\xi = 0.01$ at frequency $f = 2$ Hz, based on seismic measurements (Fig. 4). The value of the attenuation coefficient ξ at selected frequency $f = 50$ Hz was optimized through the use of scale factor s, to achieve best fit between the measured and computed maximal values of the horizontal accelerations at a few control points. As a result the damping coefficient $\xi(50\text{ Hz}) = 0.01$ and scale factor $s = 3$, were found as optimal. A comparison of the computed and measured (3 series) maximal amplitudes of horizontal accelerations is shown in Fig. 7.

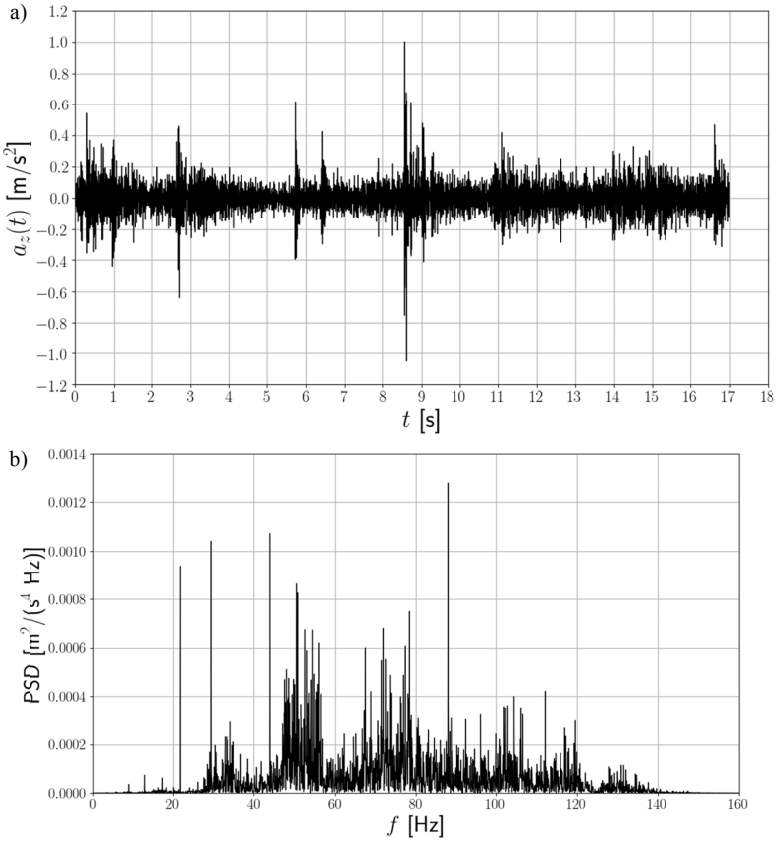

Fig. 6.Vertical acceleration $a_z(t)$ registered in the source of a working drilling rig in the reference site (after low pass Butterworth filtering (120 Hz)) (a) and its corresponding power spectrum density (PSD) (b)

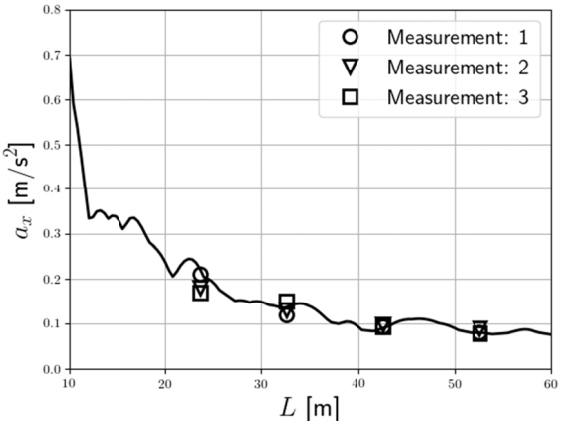

Fig. 7. Comparison of computed (continuous line) and measured (dots) maximal horizontal acceleration induced by the drilling rig at the reference site. Computed values were obtained for s = 3.0 and ξ(50 Hz) = 0.01

3.3. Modelling of ground vibrations generated by the drilling rig in the ZL design site

In the design site, the geological medium consists of: silty clay of about 0-3.6 m, clayey sand of about 3.7-11.5 m, krakowiecki clays of about 11.6-22 m and deeper shales. The results of seismic refraction measurements also indicated a horizontal and undisturbed course of seismic borders (Report, 2012). The dynamic parameters of geological layers and concrete plates in the design site are presented in Table 2.

TABLE 2

Parameters of geological layers and concrete plate in the design site (ZL)

No. of layer	Type of material	E [MPa]	ν [-]	γ [kN/m^3]	α_o [1/s]	β_o [s]
1	Silty clay	95.5	0.487	19	0.241	$6.12 \cdot 10^{-5}$
2	Clayey sand	164.1	0.488	18	0.241	$6.12 \cdot 10^{-5}$
3	Krakowiecki clays	472.7	0.488	21	0.241	$6.12 \cdot 10^{-5}$
4	Concrete plate	30000	0.2	25	0.241	$6.12 \cdot 10^{-5}$

On the basis of geological and geotechnical data, a numerical model was constructed for the conditions of the design site (Fig. 8). The boundary conditions of the model were assumed as for the model in the reference site. The estimated quadrilateral element size is equal to $h = 0.15$ m, in layers 1 and 2, and $h = 0.3$ m in layer 3, respectively. The time step, similarly to the case of the reference site, was equal to $\Delta t = 0.0009765$ s. The HHT scheme was used to integrate equations of motion in the time domain.

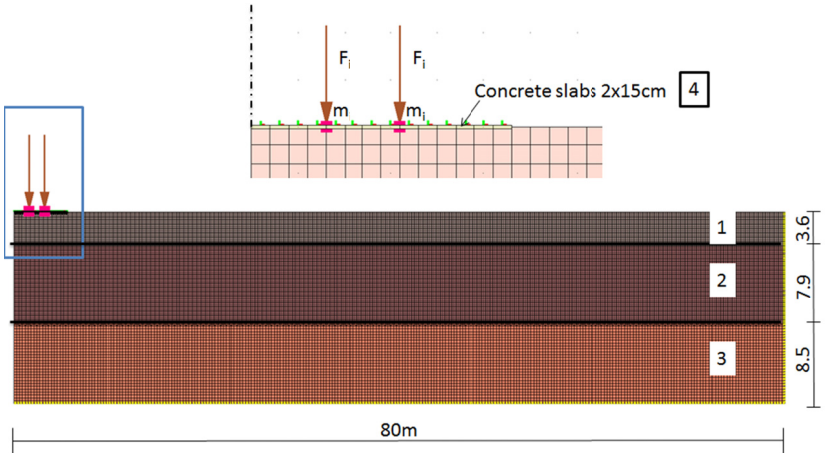

Fig. 8. Geometry of axisymmetric model with applied forces for the ZL design site

The applied scaled signal $a_z(t)$ is equivalent to the one identified at the reference site. On the basis of results of seismic tests at both sites one may conclude that the attenuation coefficients are similar. Therefore, the same values of the damping ratios were applied at the design

site (ξ (f = 2 Hz) = 0.01 and ξ (f = 50 Hz) = 0.01) (Report, 2012). Due to the fact that greater values of accelerations (about 0.2 m/s^2 at the distance of 20 m) were obtained at the design site, a vibroisolation protection system was considered. In the FE simulations that were carried out, vibroisolation pillows were used at the points of applied nodal forces. The material constants of CIBATUR vibroisolation (Calenberg web page) pillows are given in Table 3.

TABLE 3

Parameters of the vibroisolation pillow (http://www.calenberg-ingenieure.com)

Type of material	E [MPa]	ν [-]	γ [kN/m^3]	α_o [1/s]	β_o [s]
CIBATUR pillow	0.6 (s_n = 50 kN/m^2) 1.2 (s_n =100 kN/m^2)	0	4.2	0.466	$2.34 \cdot 10^{-4}$

Some preliminary estimations indicated that the contact pressure for the pillows is in the range 40-50 kN/m^2. This is important because the stiffness of the vibroisolation pillows goes up with increasing contact pressure value. Therefore, three models were analyzed i.e. a model without vibroisolation presented in Fig. 8, a model with a 3 cm thick vibroisolation pillow and assumed contact pressure σ_n = 50 kN/m^2, shown in Fig. 9, and a model with a 3 cm thick vibroisolation pillow and assumed contact pressure σ_n = 100 kN/m^2, the same as the one shown in Fig. 9.

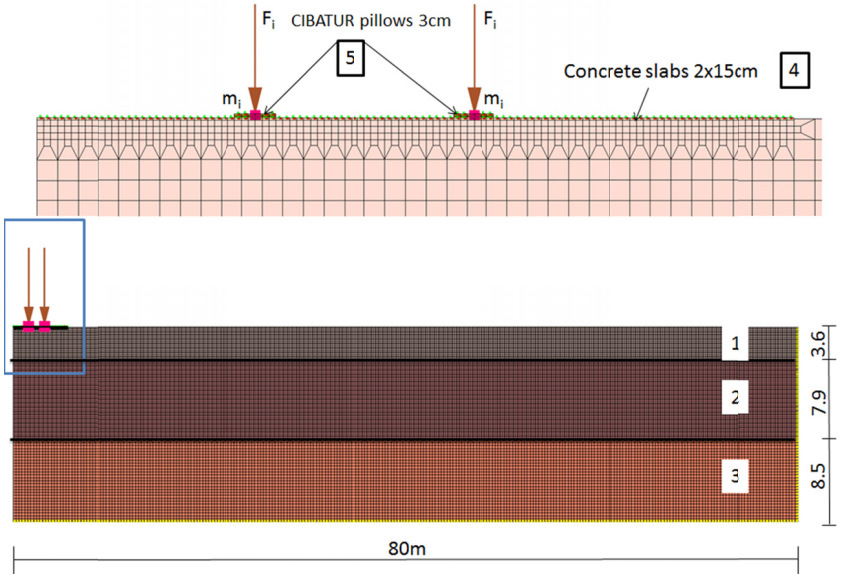

Fig. 9. Geometry of the axisymmetric model with 3 cm vibroisolation pillows for the ZL design site

The results of the simulations, presented in the form of the variation of maximum amplitude of horizontal accelerations with the increasing distance from the drilling rig, are shown in Fig. 10, for the model with contact pressure σ_n = 100 kN/m^2, and in Fig. 11 for the model with contact pressure σ_n = 50 kN/m^2. It is clearly visible that at a distance greater than 20 m (for the

model with contact pressure σ_n = 50 kN/m^2) induced vibrations are reduced at least by a factor of two. Moreover, at distances greater than 20 m maximum amplitudes are lower than 0.05 m/s^2.

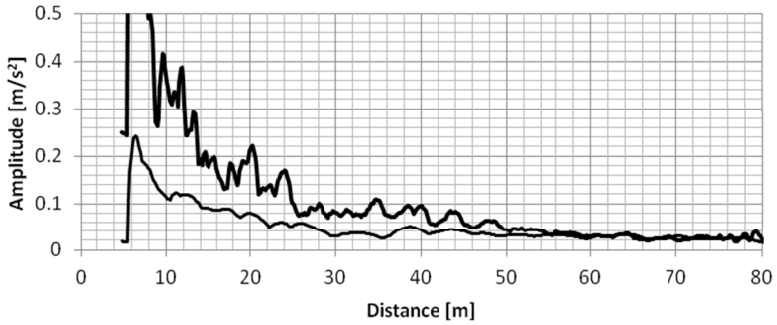

Fig. 10. Variation of maximal amplitudes of horizontal acceleration as a function of the distance from the drilling rig, for two cases: without vibroisolation pillow (thick line) and with vibroisolation pillow (thin line) (assumed contact pressure σ_n = 100 kN/m^2)

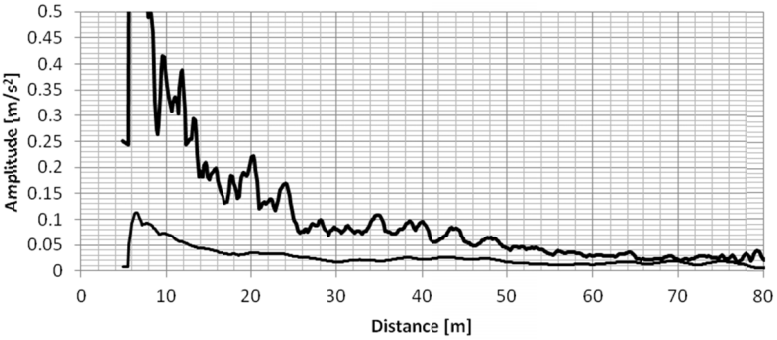

Fig. 11. Variation of maximal amplitudes of horizontal acceleration as a function of distance from the drilling rig, for the two cases: without vibroisolation pillow (thick line) and with vibroisolation pillow (thin line) (assumed contact pressure σ_n = 50 kN/m^2)

3.4. Analysis of the influence of ground vibrations induced by the drilling rig on selected segments of the mine installation

A selected segment of the mine installation, shown in Fig. 12, was analyzed with the aid of the DRM method. The two computed axisymmetric free field motions corresponding to the model with the vibroisolation system (two assumed values of the contact pressure σ_n = 50 kN/m^2 and σ_n = 100 kN/m^2) were analyzed. For an assessment of the influence of vibrations on the mechanical state of the installation segment, the envelope of bending moments was post processed. The resulting envelopes, obtained for the free field motion corresponding to the case of assumed contact pressure σ_n =100 kN/m^2, indicate that the maximum value of the bending moment M_Z (Z – vertical axis) (see Fig. 13) is equal to 0.107 kNm, and M_Y (Y – radial axis) is

equal to 0.084 kNm. These values are acceptable from the installation stability point of view. Results corresponding to the case of a contact pressure σ_n = 50 kN/m^2 pointed to negligible differences, not larger than 5%.

The analyses indicated the absolute need of the application of the vibroisolation system. In the analyzed cases, the application of 3 cm thick CIBATUR vibroisolation pillows leads to a sufficient reduction of harmful vibrations at a distance greater than 20 m.

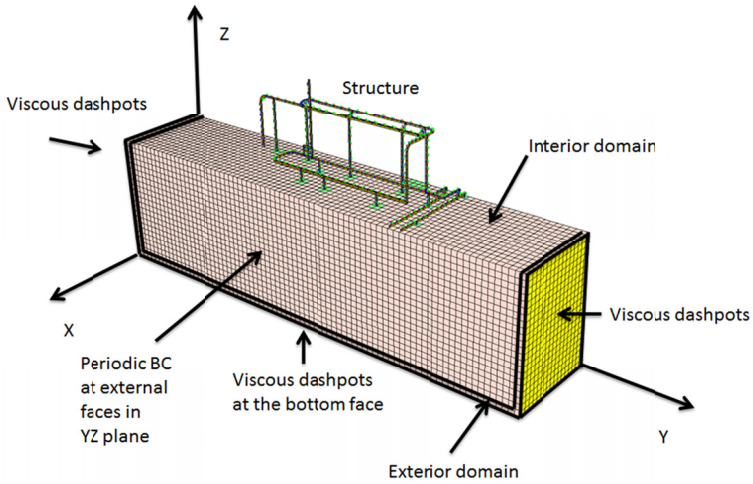

Fig. 12. Reduced 3D model with mine installation segment

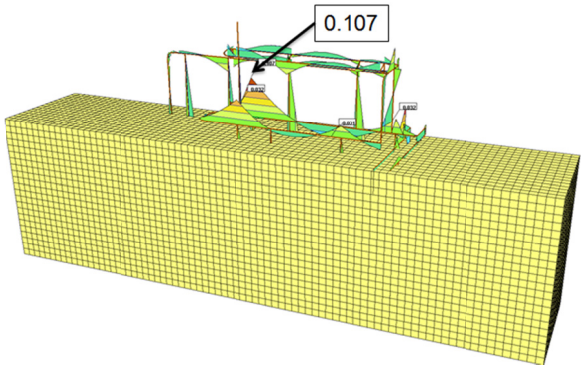

Fig. 13. Envelope of bending moment M_z obtained for the free field motion corresponding to the vibroisolation system at assumed contact pressure σ_n = 50 kN/m^2 (greatest moment is of the order of 0.107 kNm)

4. Summary

In the study, a methodology based on the Domain Reduction Method of FEM to analyze ground vibrations induced by working drilling rigs was proposed. It allows for the estimation of

ground vibrations, before a given drilling rig is installed in the design site. In order to analyze it, one should measure the parameters of ground vibrations induced by a given type of drilling system in the reference site. After that, ground vibrations are modeled in a design site for the same drilling system as a vibration source. In both sites special seismic investigations are conducted to obtain the dynamic parameters of the near surface medium and its structure. The simplified axisymmetric FEM simulations of the free field motion and then detailed analyses of selected engineering structures, carried out with the help of the DRM method, allows the safe distance of the drilling rig from neighboring structures to be determined. If necessary, an efficient vibroisolation protection system may be proposed for a given drilling rig and local conditions. In the presented simulation, the application of vibroisolation pillows of 3 cm thickness caused a sufficient reduction in harmful vibrations at distances greater than 20 m.

It is clear that our numerical simulation is based on simplified models of subsoil and drilling rig, as a source of vibrations, therefore, the obtained results should be verified by control measurements. Based on the results of our research we conclude that:

- the proposed methodology allows for the location of a drilling system that preserves sufficient safety for the surrounding engineering structures,
- if necessary, we can design an effective vibroisolation system to decrease the unfavorable vibrations.
- the proposed methodology may be used to assess the impact of a working drilling rig on humans and the natural environmental. This may be crucial in solving environmental and social problems in the neighborhood of urban areas.

References

Angona F., 1965. *Drill string vibrations attenuation and its effect on a surface oscillator drilling system*. Journal of Engineering for Industry, Transaction of the ASME **87**, 2, 110-114.

Bailey J.J., Finnie I., 1960. *An analytical study of drillstring vibration*. Journal of Engineering for Industry, Transactions of the ASME **82** (2), 122-128.

Bailey J.R., Biediger E., Gupta V., Ertas D., Elks W.C., Dupriest F.E., 2008. *Drilling vibrations modeling and field validation*. Proc. IADC/SPE Drilling Conference, 4-6 March, Orlando, Florida, USA, doi:10.2118/112650-MS

Bielak J., Laukakis K., Hisada V., Youshimura C., 2003. *Domain reduction method for three-dimensional earthquake modeling in localized regions*. Part I: Theory. Bulletin of the seismological Society of America **93** (2), 817-824.

Cunningham R., 1968. *Analyzis of downhole measurements of drill string forces and motions*. Journal of Engineering for Industry, Transactions of the ASME **90**, 2, 208-216.

Hilber H.M., Hughes T.J.R., Taylor R.L., 1977. *Improved numerical dissipation for time integration algorithms in structural dynamics*. Earthquake Eng. And Struc. Dyn. **5**, 283- 292.

Finnie I., Bailey J.J. 1960. *An experimental study of drill-string vibration*. Journal of Engineering for Industry, Transactions of the ASME **82** (2), 129-135.

Jardine S., Malone D., Sheppard M., 1994. *Putting a damper on drilling,s bad vibrations*. Oilfield Review **1**, 15-20.

Miller L.E., Rollins H.M., 1968. *Evaluation of vibration damping tool and of drill stem torque requirements from data recorded by an instrumented drill stem member*. ASME J. of Eng. for Ind., 226-230.

Nicholls K., 2009. *Estimating the potential impact of cable percussion piling* – Technical note. Ground Engineering, October 2009, 44-45.

Saldivar B., Boussaada I., Mounier H., Mondi´e S., Niculescu S.I., 2014. *An Overview on the Modeling of Oilwell Drilling Vibrations*. Preprints of the 19th World Congress The International Federation of Automatic Control Cape Town, South Africa. August 24-29, 2014.

Saldivar Marquez M.B., Boussaada I., Mounier H., Niculescu S.I., 2015. *Analysis and Control of Oilwell Drilling Vibrations – A Time-Delay Systems Approach*. Series: Advances in Industrial Control 2015, XXIII, 282 p. 86 illus. Springer.

Spanos D., Chevallier A.M., Politis N.P., Payne M.L., 2003. *Oil and Gas Well Drilling: A Vibrations Perspective*. The Shock and Vibration Digest 03/2003; 35(2):85-103. DOI: 10.1177/0583102403035002564

Stypula K., 1981. *The study of propagation vibrations in the ground generated by driving of foundation piles*. PhD thesis. Cracow University of Technology, Kraków (in Polish).

Truty A., Zimmermann Th., 2013. *Domain reduction method for single and two-phase dynamic soil-structure interaction problems*. Proceedings of the 3rd I International Symposium on Computational Geomechanics (COMGEO III), Krakow, Poland, 21-23 August, 2013, 273-283.

Youshimura C., Bielak J., Hisada Y., Fernandez A., 2003. *Domain reduction method for three-dimensional earthquake modeling in localized regions Part II: Verification and applications*. Bulletin of the Seismological Society of America **93** (2), 825-840.

Web pages

http://www.calenberg-ingenieure.com

Truty A., Zimmermann T., 2013. *Dynamics in ZSoil.* PC. Report 130101. Zace Services Limited. (web page: www.zsoil.com)

APPENDIX 1

GOVERNING EQUATIONS OF MOTION IN THE DOMAIN REDUCTION METHOD

In the Domain Reduction Method the whole domain is partitioned into the interior domain Ω (small zone of subsoil adjacent to the structure and the structure itself) and the exterior domain Ω^+ (remaining part of the subsoil). Nodes in the FE mesh that belong exlusively to the interior domain are labeled with an index i, nodes in the exterior domain with an index e, and nodes at the interface between the interior and exterior domains with an index b. Standard semi-discrete equations of motion for an elastic continuum and structure, written separately in Ω (eq. A1.1) and Ω^+ (eq. A1.2) are as follows (to avoid excessive derivations damping terms are neglected here but adding them is straightforward):

$$\begin{bmatrix} \mathbf{M}_{ii}^{\Omega} & \mathbf{M}_{ib}^{\Omega} \\ \mathbf{M}_{bi}^{\Omega} & \mathbf{M}_{bb}^{\Omega} \end{bmatrix} \begin{Bmatrix} \ddot{\mathbf{u}}_i \\ \ddot{\mathbf{u}}_b \end{Bmatrix} + \begin{bmatrix} \mathbf{K}_{ii}^{\Omega} & \mathbf{K}_{ib}^{\Omega} \\ \mathbf{K}_{bi}^{\Omega} & \mathbf{K}_{bb}^{\Omega} \end{bmatrix} \begin{Bmatrix} \mathbf{u}_i \\ \mathbf{u}_b \end{Bmatrix} = \begin{Bmatrix} \mathbf{0} \\ \mathbf{P_b} \end{Bmatrix} \tag{A1.1}$$

$$\begin{bmatrix} \mathbf{M}_{bb}^{\Omega^+} & \mathbf{M}_{be}^{\Omega^+} \\ \mathbf{M}_{eb}^{\Omega^+} & \mathbf{M}_{ee}^{\Omega^+} \end{bmatrix} \begin{Bmatrix} \ddot{\mathbf{u}}_b \\ \ddot{\mathbf{u}}_e \end{Bmatrix} + \begin{bmatrix} \mathbf{K}_{bb}^{\Omega^+} & \mathbf{K}_{be}^{\Omega^+} \\ \mathbf{K}_{eb}^{\Omega^+} & \mathbf{K}_{ee}^{\Omega^+} \end{bmatrix} \begin{Bmatrix} \mathbf{u}_b \\ \mathbf{u}_e \end{Bmatrix} = \begin{Bmatrix} -\mathbf{P}_b \\ \mathbf{P}_e \end{Bmatrix} \tag{A1.2}$$

The $\mathbf{P_b}$ term represents boundary forces, that appear due to the partitioning procedure, while $\mathbf{P}_e$ is the source of vibrations. The corresponding mass and stiffness matrices are denoted by $\mathbf{M}$ and $\mathbf{K}$, while nodal displacements and accelerations are indicated by $\mathbf{u}$ and $\ddot{\mathbf{u}}$ respectively.

The two sets of equations above can be written in the global form as follows:

$$\begin{bmatrix} \mathbf{M}_{ii}^{\Omega} & \mathbf{M}_{ib}^{\Omega} & \mathbf{0} \\ \mathbf{M}_{bi}^{\Omega} & \mathbf{M}_{bb}^{\Omega}+\mathbf{M}_{bb}^{\Omega^+} & \mathbf{M}_{be}^{\Omega^+} \\ \mathbf{0} & \mathbf{M}_{eb}^{\Omega^+} & \mathbf{M}_{ee}^{\Omega^+} \end{bmatrix} \begin{Bmatrix} \ddot{\mathbf{u}}_i \\ \ddot{\mathbf{u}}_b \\ \ddot{\mathbf{u}}_e \end{Bmatrix} + \begin{bmatrix} \mathbf{K}_{ii}^{\Omega} & \mathbf{K}_{ib}^{\Omega} & \mathbf{0} \\ \mathbf{K}_{bi}^{\Omega} & \mathbf{K}_{bb}^{\Omega}+\mathbf{K}_{bb}^{\Omega^+} & \mathbf{K}_{be}^{\Omega^+} \\ \mathbf{0} & \mathbf{K}_{eb}^{\Omega^+} & \mathbf{K}_{ee}^{\Omega^+} \end{bmatrix} \begin{Bmatrix} \mathbf{u}_i \\ \mathbf{u}_b \\ \mathbf{u}_e \end{Bmatrix} = \begin{Bmatrix} \mathbf{0} \\ \mathbf{0} \\ \mathbf{P_e} \end{Bmatrix} \tag{A1.3}$$

By decomposing the displacement vector in the exterior domain $\mathbf{u}_e$ into free field displacement $\mathbf{u}_e^0$ and the residual one $\hat{\mathbf{u}}_e$ (same decomposition applies to the velocities and accelerations):

$$\mathbf{u}_e = \mathbf{u}_e^0 + \hat{\mathbf{u}}_e \tag{A1.4}$$

the eq. (A1.3) can be rewritten in the following form:

$$\begin{bmatrix} \mathbf{M}_{ii}^{\Omega} & \mathbf{M}_{ib}^{\Omega} & \mathbf{0} \\ \mathbf{M}_{bi}^{\Omega} & \mathbf{M}_{bb}^{\Omega}+\mathbf{M}_{bb}^{\Omega^+} & \mathbf{M}_{be}^{\Omega^+} \\ \mathbf{0} & \mathbf{M}_{eb}^{\Omega^+} & \mathbf{M}_{ee}^{\Omega^+} \end{bmatrix} \begin{Bmatrix} \ddot{\mathbf{u}}_i \\ \ddot{\mathbf{u}}_b \\ \ddot{\hat{\mathbf{u}}}_e \end{Bmatrix} + \begin{bmatrix} \mathbf{K}_{ii}^{\Omega} & \mathbf{K}_{ib}^{\Omega} & \mathbf{0} \\ \mathbf{K}_{bi}^{\Omega} & \mathbf{K}_{bb}^{\Omega}+\mathbf{K}_{bb}^{\Omega^+} & \mathbf{K}_{be}^{\Omega^+} \\ \mathbf{0} & \mathbf{K}_{eb}^{\Omega^+} & \mathbf{K}_{ee}^{\Omega^+} \end{bmatrix} \begin{Bmatrix} \mathbf{u}_i \\ \mathbf{u}_b \\ \hat{\mathbf{u}}_e \end{Bmatrix} =$$

$$= \begin{Bmatrix} \mathbf{0} \\ -\mathbf{M}_{be}^{\Omega^+}\ \ddot{\mathbf{u}}_e^0 - \mathbf{K}_{be}^{\Omega^+}\ \mathbf{u}_e^0 \\ \mathbf{P_e} - \mathbf{M}_{ee}^{\Omega^+}\ \ddot{\mathbf{u}}_e^0 - \mathbf{K}_{ee}^{\Omega^+}\ \mathbf{u}_e^0 \end{Bmatrix} \tag{A1.5}$$

The $\mathbf{P}_e$ term can now be derived from eq. (A1.2) assuming that it is solved for a simpler problem that does not include the structure, which yields:

$$\mathbf{P}_e = \mathbf{M}_{eb}^{\Omega^+}\ddot{\mathbf{u}}_b^0 + \mathbf{M}_{ee}^{\Omega^+}\ddot{\mathbf{u}}_e^0 + \mathbf{K}_{eb}^{\Omega^+}\mathbf{u}_b^0 + \mathbf{K}_{ee}^{\Omega^+}\mathbf{u}_e^0 \tag{A1.6}$$

By substituting the above $\mathbf{P}_e$ term into eq. (A1.5) the following form of the right hand side vector $\mathbf{P}^{eff}$ is obtained:

$$\mathbf{P}^{eff} = \begin{Bmatrix} \mathbf{0} \\ -\mathbf{M}_{be}^{\Omega^+}\ \ddot{\mathbf{u}}_e^0 - \mathbf{K}_{be}^{\Omega^+}\ \mathbf{u}_e^0 \\ \mathbf{M}_{eb}^{\Omega^+}\ \ddot{\mathbf{u}}_b^0 + \mathbf{K}_{eb}^{\Omega^+}\ \mathbf{u}_b^0 \end{Bmatrix} \tag{A1.7}$$

It is clear that the nonzero terms in the right hand side vector appear exlusively at the nodes of the elements in the boundary layer.